The lightest D_0^* resonance from lattice QCD

Nicolas Lang[*]

School of Mathematics and Hamilton Mathematics Institute, Trinity College, Dublin 2, Ireland

E-mail: nicolas.lang@maths.tcd.ie

We recently presented elastic $I = 1/2$ $D\pi$ scattering from lattice QCD at $m_\pi = 239$ MeV. The amplitude features a pole corresponding to a mass $m \approx 2200$ MeV and a width $\Gamma \approx 400$ MeV. The results were compared to an earlier study at a higher pion mass and to a similar study in the charm-strange sector. In this contribution to LATTICE2021 I summarize these results and compare them with experiment, based on the values reported by the particle data group. Our result lies significantly below the experimental D_0^*. I also relate our findings to recent studies in chiral perturbation theory.

The 38th International Symposium on Lattice Field Theory, LATTICE2021 26th-30th July, 2021
Zoom/Gather@Massachusetts Institute of Technology

---

[*]Speaker

1. Introduction

Open-charm systems are an interesting testing ground for our understanding of low-energy QCD. The lightest scalar charm-light state D_0^* and its relation to the corresponding charm-strange state D_{s0}^* has been a puzzle since the experimental discovery of the two mesons in 2003. From the perspective of the quark-model both states are represented by the scalar arising from a charm- and a light- or strange-quark interacting in a relative *P*-wave. The mass difference of the two states is therefore expected to be due, in large part, to the difference of the light and strange quark masses. However, the current particle data group (PDG) average [1, 2] locates the D_0^* at an energy compatible with that of the D_{s0}^*, as shown in fig. 1.1. The large width of the D_0^* that was found experimentally furthermore casts doubt on the validity of the quark model results for this system.

As a model independent approach, lattice QCD allows for the study of hadron resonances as they arise purely from QCD dynamics. While the current technical requirement to perform most calculations at larger-than-physical quark masses may be seen as a limitation, it can also be regarded as a tool to map out the quark mass dependence of the states between the flavour symmetric point and the physical mass. In this contribution, I summarize the results from our recent study of $I = 1/2$ $D\pi$ scattering [3], which completes a quartet of studies of the scalar charm-light and charm-strange sector at two different mass points [4, 5]. I also relate our results to recent studies in unitarised chiral perturbation theory and present an outlook for future investigations.
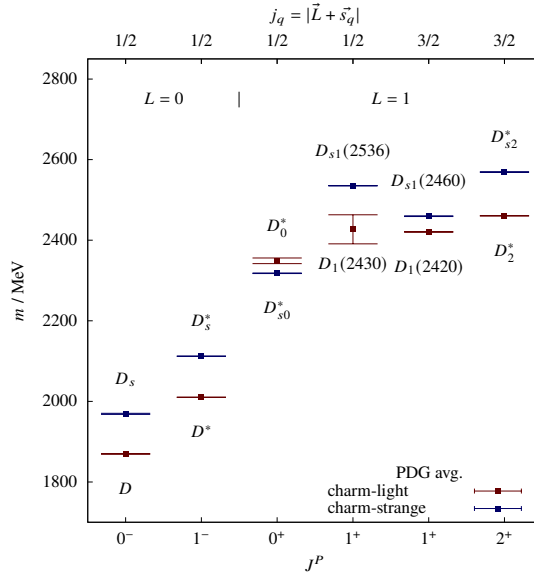

Figure 1.1: Average mass values reported by the PDG [1, 2] of the lowest charm-light and charm-strange states. The bottom horizontal axis shows the total angular momentum and parity J^P whereas the top horizontal axis indicates the magnitude of the sum j_q of the orbital angular momentum $\vec{L}$ and light-/strange-quark spin $\vec{s}_q$ of the corresponding quark-model state. The two quark spins are conserved separately in the heavy-quark limit.

2. Lattice Calculation

The calculation is performed on an $(L/a_s)^3 \times (T/a_t) = 32^3 \times 256$ anisotropic lattice with 2+1 dynamical quark flavours, L and T denoting the spatial and temporal lattice extents respectively, and a_s (a_t) the spatial (temporal) lattice spacing. The anisotropy $\xi \equiv a_s/a_t \approx 3.5$ and the stable hadron masses are obtained from a fit of the relativistic dispersion relation

$$(a_t E)^2 = (a_t m)^2 + \vec{d}^2 \left(\frac{2\pi}{\xi \, L/a_s} \right)^2 \tag{1}$$

to the lattice energies of the respective hadron at different momenta. Here $\vec{d}$ is a vector of integers pointing in the momentum direction. We use the ξ value from the pion fit in this calculation to convert energies to the rest-frame, but consider the D meson anisotropy in the assessment of systematic uncertainties. The scale setting is done through a comparison of the calculated Ω baryon mass on this ensemble with the physical one, such that $a_t^{-1} = m_\Omega^{\text{phys.}}/a_t m_\Omega^{\text{lat.}}$. The ensemble was generated using a tree-level Symanzik-improved anisotropic action in the gauge sector and a tree-level, tadpole-improved Sheikholeslami-Wohlert action for the fermions. The light quarks are heavier-than-physical while the strange quark is tuned to approximate the physical value. Table 1 summarises the most relevant properties of the ensemble.

a_s	a_t^{-1}	$(L/a_s)^3 \times (T/a_t)$	m_π	N_f	N_{cfg}
0.11 fm	6.079 GeV	$32^3 \times 256$	239 MeV	$2+1$	484

Table 1: Ensemble used in the calculation

Correlators are computed using the distillation framework [6]. All relevant graphs are evaluated, including disconnected pieces. The spectrum is obtained from a variational analysis of correlation functions obtained from a basis of interpolating operators, including $q\bar{q}$-like and meson-meson-like operators, solving the generalised eigenvalue equation

$$C_{ij}(t) v_j^{(n)} = \lambda_n(t, t_0) C_{ij}(t_0) v_j^{(n)}, \tag{2}$$

where $C_{ij}(t)$ is the matrix of correlators. Operators are projected to irreducible representations (*irreps*) of the cubic group O_h (at rest) and the little group $LG(\vec{p})$ at non-zero momentum to allow for the recovery of angular momentum information from the lattice spectra. To obtain scattering amplitudes in the infinite volume we utilise the Lüscher quantisation condition [7–9] and its extensions [10–18], which allows a fit of a parametrised t-matrix to the energy levels calculated in the finite volume. In our reference fit we parameterise the t-matrix as

$$(t^{(\ell)})^{-1}(s) = \frac{1}{(2k)^\ell} K^{-1}(s) \frac{1}{(2k)^\ell} + I(s)$$

$$K(s) = \frac{g^2}{m^2 - s} + \gamma \, . \tag{3}$$

$I(s)$ denotes the Chew-Mandelstam phase space subtracted at the energy of the pole parameter, $k(s)$ is the momentum in the center-of-momentum frame as a function of Mandelstam s and m, g and γ are free parameters. To estimate the uncertainty arising from the choice of the specific functional

form of the t matrix, we fit a range of different parametrisations, among them different K-matrix forms, effective range and scattering length parametrisations as well as a Breit-Wigner. We also consider an amplitude based on unitarised chiral perturbation theory [19].

3. Results

We compute spectra for 10 irreps, both at rest and with one, two and three units of momentum. Figure 3.1 shows a subset of these. We perform an S-wave fit based on 20 energy levels from 5 irreps where $l = 0$ is the leading partial wave. There is a small but non-zero P-wave contribution in the moving-frame irreps, which we consider including a pole term in the K-matrix, accounting for an extra energy level far below $D\pi$ threshold appearing in these irreps. Using a single energy level from the E^+ irrep we show that the D-wave phase shift is consistent with zero and we therefore conclude that higher partial waves can be neglected. The energy levels used in the fit are all below the threshold where three-body $D\pi\pi$ scattering becomes kinematically possible and therefore, at this mass point, well below other thresholds of inelastic scattering. For the fit of our reference amplitude, using the K-matrix given by eq. 3 in the S wave channel, we obtain $\chi^2/N_{\text{dof}} = \frac{13.49}{20-5} = 0.90$.

We analytically continue amplitudes to complex values of Mandelstam-s. Above $D\pi$ threshold there are two Riemann sheets due to the multi-particle branch cut, which are referred to as physical and unphysical sheet. Physical scattering occurs above the real axis on the physical sheet. Poles of the amplitude on the unphysical sheet may be interpreted as resonances and their residue gives the coupling to the decay channel. While the fits constrain the behaviour on the real axis, there may be large differences between parametrisations at complex energies. The amplitudes we consider are analytic, except for poles and the multi-particle branch cut along the real axis. Using the K-matrix formalism, they obey the constraint of unitarity by construction. We also aim to preserve causality by rejecting amplitudes that feature nearby poles above threshold on the physical sheet. The remaining amplitudes consistently feature an S wave pole approximately 77 ± 64 MeV above threshold, with an imaginary part between 200 and 600 MeV, indicating a resonance as a universal feature. For the pole and its residue we obtain the estimate

$$\sqrt{s_0}/\text{MeV} = (2196 \pm 64) - \tfrac{i}{2}(425 \pm 224)$$
$$c/\text{MeV} = (1916 \pm 776)\exp i\pi(-0.59 \pm 0.41)$$

from an envelope around the poles of all amplitude variations. We also take into account variations of the stable hadron masses and the anisotropy within their uncertainties, which are inputs to the Lüscher determinant condition. The amplitude (pole) resulting from our fits corresponds to the red curve (data point) in the left (right) panel of fig. 4.1. The corresponding solutions of the Lüscher determinant condition yielding the finite volume energy levels are superimposed onto the spectrum in fig. 3.1.
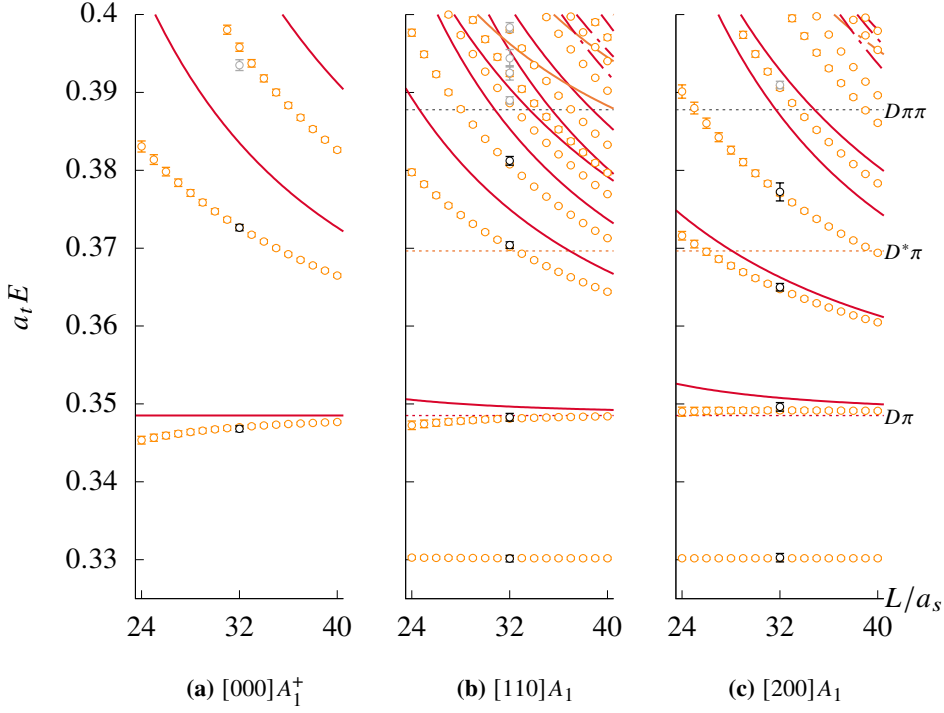
Figure 3.1: The finite volume spectrum in three of the irreps used to constrain the $D\pi$ S-wave amplitude. Black data points and error bars represent the energies obtained from the lattice. Dotted lines indicate thresholds. Solid lines correspond to non-interacting energies of operators included in the variational analysis. The solutions of the Lüscher determinant condition based on our reference amplitude parametrisation are superimposed in orange. (From fig. 5 and 6 in [3])

4. Interpretation

Despite a heavier-than-physical pion mass, our result for the D_0^* mass lies significantly below the experimental value reported by the PDG, which is approximately 2350 MeV. It is interesting to note that the real part of the pole location is far from the point where the amplitude touches the unitarity bound (see fig. 4.1). This difference is also reflected in our Breit-Wigner fit: whereas the pole of the Breit-Wigner amplitude is in agreement with our K matrix result, the mass parameter of the amplitude takes on a value of 2380 ± 36 MeV, compatible with the PDG value.

Mass dependence

An earlier study of $D\pi$ scattering [4] was conducted on an ensemble with a heavier pion mass m_π = 391 MeV, whereas the ensemble used in our present study corresponds to m_π = 239 MeV. This allows at least for the identification of a trend in the mass dependence of the amplitude. Fig. 4.1 shows the S-wave amplitudes and their poles obtained on both ensembles. At the larger mass a shallow bound state was found just 2 ± 1 MeV below $D\pi$ threshold, which migrates into the complex plane at m_π = 239 MeV. Both amplitudes turn on rapidly above threshold indicating a large coupling to $D\pi$, which is reflected in the residue of the pole (see the bottom part of the right panel of fig. 4.1).
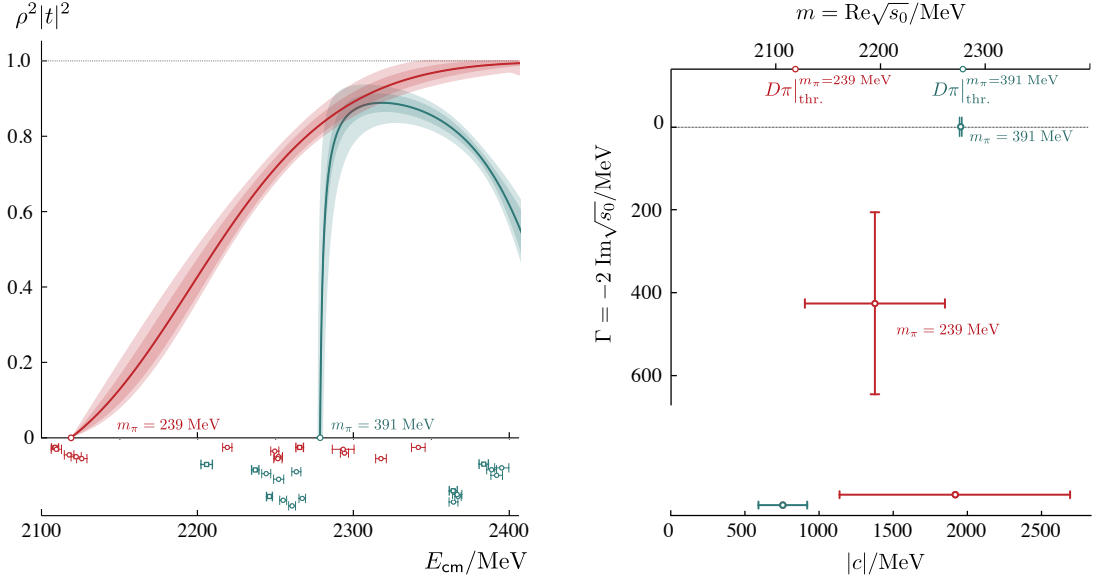
Figure 4.1: Comparison of the S-wave amplitudes (left panel), poles (right panel, top) and magnitude of couplings (right panel, bottom) at two different mass points. Energy levels constraining the amplitudes are indicated below the plot in the left panel. The inner bands around the amplitudes indicate the statistical uncertainty on the parameter values resulting from the fit. For $m_\pi = 239$ MeV the outer band includes variations of the hadron masses, anisotropy and parametrisation, for $m_\pi = 391$ MeV only variations of masses and anisotropy are included. (Fig. 10 in [3])

Comparison to DK

As mentioned in the introduction, it is illuminating to compare the $D\pi$ system to the closely related DK system. In [5] DK scattering amplitudes were calculated at both of the above-mentioned pion masses. We summarize the real parts of the poles extracted from the S-wave amplitudes at the two mass points for $I = 1/2$ $D\pi$ and $I = 0$ DK in fig. 4.2. The shallow $D\pi$ bound state at the higher pion mass evolves into a broad near-threshold resonance at the lower mass, while the DK pole remains bound at both masses, showing only a very slight quark mass dependence. But clearly, the mass hiararchy of the two systems expected from the difference of the light and strange quark masses remains the same. From the observed trend we would expect a resonant D_0^* at the physical point whereas it is unclear whether the D_{s0}^* would remain bound or evolve into a near-threshold resonance.

Comparison to $\chi_{\mathbf{PT}}$ results

In the limit where $m_u = m_d = m_s$ the t matrix for open-charm scattering can be decomposed in terms of the irreps of $SU(3)_\mathrm{F}$ as $\overline{\mathbf{3}} \otimes \mathbf{8} = \overline{\mathbf{15}} \oplus \mathbf{6} \oplus \overline{\mathbf{3}}$. Using unitarised chiral perturbation theory, it was shown in [20] that the anti-triplet pole splits into two when evolved in mass away from the $SU(3)$ limit towards the physical point. The mass evolution shown in Fig. 5 of the referenced work is roughly compatible with the poles obtained on our ensembles, when adjusting for the scale setting, suggesting that the D_0^* and D_{s0}^* correspond to the same $SU(3)_\mathrm{F}$ multiplet. The mass evolution of the sextet state implies that the D_0^* amplitude might feature an additional pole at a higher energy.
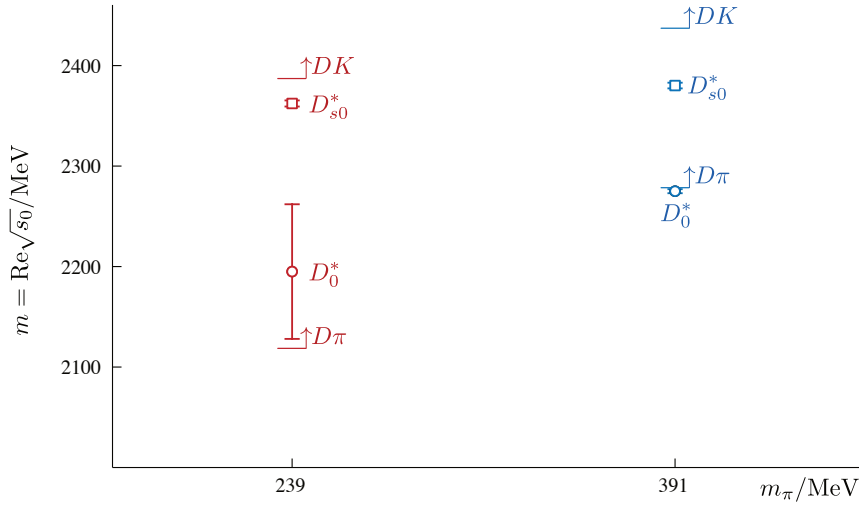
Figure 4.2: The real parts of the *S*-wave amplitude pole locations for $D\pi$ and DK scattering at two different pion masses. The respective kinematic thresholds are indicated. (Fig. 13 in [3])

The contribution by Guo et. al. [21] to LATTICE2021 makes a strong case for the existence of this pole. They perform a global fit including data obtained from the lattice for $m_\pi \approx 391$ MeV and predict the energy dependence of the phase shift for $m_\pi \approx 239$ MeV, which shows good agreement with our result close to $D\pi$ threshold.

Outlook

Supporting the existence of the higher pole from the lattice side will require more data and the inclusion of the coupled channel in the scattering analysis. This could be an interesting future investigation. Additionally it would be worthwhile to perform this study at further pion masses, providing constraints on the mass evolution predicted by chiral perturbation theory. Lastly, a similar set of open-charm axial-vector states is predicted and a corresponding analysis performed in the $D^*\pi$ and D^*K channels would allow for a comparison.

Acknowledgements

References

[1] M. Tanabashi et al. Review of particle physics. *Phys. Rev. D*, 98:030001, Aug 2018.

[2] Particle Data Group, P A Zyla, et al. Review of Particle Physics. *Progress of Theoretical and Experimental Physics*, 2020(8), 08 2020. 083C01.

[3] Luke Gayer, Nicolas Lang, Sinéad M. Ryan, David Tims, Christopher E. Thomas, and David J. Wilson. Isospin-1/2 $d\pi$ scattering and the lightest D_0^* resonance from lattice qcd. *Journal of High Energy Physics*, 2021(7), Jul 2021.

7

[4] Graham Moir, Michael Peardon, Sinéad M. Ryan, Christopher E. Thomas, and David J. Wilson. Coupled-Channel $D\pi$, $D\eta$ and $D_s\bar{K}$ Scattering from Lattice QCD. *JHEP*, 10:011, 2016.

[5] Gavin K.C. Cheung, Christopher E. Thomas, David J. Wilson, Graham Moir, Michael Peardon, and Sinéad M. Ryan. DK $I = 0$, $D\bar{K}$ $I = 0, 1$ scattering and the $D_{s0}^*(2317)$ from lattice QCD. 8 2020.

[6] Michael Peardon, John Bulava, Justin Foley, Colin Morningstar, Jozef Dudek, Robert G. Edwards, Balint Joo, Huey-Wen Lin, David G. Richards, and Keisuke Jimmy Juge. A Novel quark-field creation operator construction for hadronic physics in lattice QCD. *Phys. Rev.*, D80:054506, 2009.

[7] M. Luscher. Volume Dependence of the Energy Spectrum in Massive Quantum Field Theories. 2. Scattering States. *Commun. Math. Phys.*, 105:153–188, 1986.

[8] Martin Luscher. Two particle states on a torus and their relation to the scattering matrix. *Nucl. Phys.*, B354:531–578, 1991.

[9] Martin Luscher. Signatures of unstable particles in finite volume. *Nucl. Phys.*, B364:237–251, 1991.

[10] K. Rummukainen and Steven A. Gottlieb. Resonance scattering phase shifts on a nonrest frame lattice. *Nucl. Phys.*, B450:397–436, 1995.

[11] C. h. Kim, C. T. Sachrajda, and Stephen R. Sharpe. Finite-volume effects for two-hadron states in moving frames. *Nucl. Phys.*, B727:218–243, 2005.

[12] Norman H. Christ, Changhoan Kim, and Takeshi Yamazaki. Finite volume corrections to the two-particle decay of states with non-zero momentum. *Phys. Rev.*, D72:114506, 2005.

[13] Ziwen Fu. Rummukainen-Gottlieb's formula on two-particle system with different mass. *Phys. Rev.*, D85:014506, 2012.

[14] Luka Leskovec and Sasa Prelovsek. Scattering phase shifts for two particles of different mass and non-zero total momentum in lattice QCD. *Phys. Rev.*, D85:114507, 2012.

[15] Maxwell T. Hansen and Stephen R. Sharpe. Multiple-channel generalization of Lellouch-Luscher formula. *Phys. Rev. D*, 86:016007, 2012.

[16] Raul A. Briceno and Zohreh Davoudi. Moving multichannel systems in a finite volume with application to proton-proton fusion. *Phys. Rev. D*, 88(9):094507, 2013.

[17] Peng Guo, Jozef Dudek, Robert Edwards, and Adam P. Szczepaniak. Coupled-channel scattering on a torus. *Phys. Rev. D*, 88(1):014501, 2013.

[18] Raul A. Briceno. Two-particle multichannel systems in a finite volume with arbitrary spin. *Phys. Rev. D*, 89(7):074507, 2014.

[19] Zhi-Hui Guo, Liuming Liu, Ulf-G Meißner, J.A. Oller, and A. Rusetsky. Towards a precise determination of the scattering amplitudes of the charmed and light-flavor pseudoscalar mesons. *Eur. Phys. J. C*, 79(1):13, 2019.

[20] Miguel Albaladejo, Pedro Fernandez-Soler, Feng-Kun Guo, and Juan Nieves. Two-pole structure of the D_0^* (2400). *Physics Letters B*, 767:465–469, Apr 2017.

[21] Xiao-Yu Guo, Yonggoo Heo, and Matthias F. M. Lutz. From lattice QCD to predictions of scattering phase shifts at the physical point. In *38th International Symposium on Lattice Field Theory*, 7 2021.

[22] Robert G. Edwards and Balint Joo. The Chroma software system for lattice QCD. *Nucl. Phys. Proc. Suppl.*, 140:832, 2005.

[23] M. A. Clark, R. Babich, K. Barros, R. C. Brower, and C. Rebbi. Solving Lattice QCD systems of equations using mixed precision solvers on GPUs. *Comput. Phys. Commun.*, 181:1517–1528, 2010.

[24] Ronald Babich, Michael A. Clark, and Balint Joo. Parallelizing the QUDA Library for Multi-GPU Calculations in Lattice Quantum Chromodynamics. In *SC 10 (Supercomputing 2010) New Orleans, Louisiana, November 13-19, 2010*, 2010.

[25] Bálint Joó, Dhiraj D. Kalamkar, Karthikeyan Vaidyanathan, Mikhail Smelyanskiy, Kiran Pamnany, Victor W. Lee, Pradeep Dubey, and William Watson. Lattice QCD on Intel® Xeon Phi Coprocessors. *Lect. Notes Comput. Sci.*, 7905:40–54, 2013.

[26] J. C. Osborn, R. Babich, J. Brannick, R. C. Brower, M. A. Clark, S. D. Cohen, and C. Rebbi. Multigrid solver for clover fermions. *PoS*, LATTICE2010:037, 2010.

[27] R. Babich, J. Brannick, R. C. Brower, M. A. Clark, T. A. Manteuffel, S. F. McCormick, J. C. Osborn, and C. Rebbi. Adaptive multigrid algorithm for the lattice Wilson-Dirac operator. *Phys. Rev. Lett.*, 105:201602, 2010.